

5-2015

Progress towards the Kinetic Characterization of PhaG, a Key Enzyme in the Biosynthesis of Poly-[(R)-3-hydroxyalkanoates] in Bacteria

John G. Ganley

Follow this and additional works at: <http://digitalcommons.esf.edu/honors>



Part of the [Chemistry Commons](#)

Recommended Citation

Ganley, John G., "Progress towards the Kinetic Characterization of PhaG, a Key Enzyme in the Biosynthesis of Poly-[(R)-3-hydroxyalkanoates] in Bacteria" (2015). *Honors Theses*. 109.
<http://digitalcommons.esf.edu/honors/109>

**Progress towards the kinetic characterization of PhaG, a key enzyme in
the biosynthesis of poly-[(R)-3-hydroxyalkanoates] in bacteria**

by

John G. Ganley
Candidate of Bachelor of Science
Department of Chemistry
With Honors

May 2015

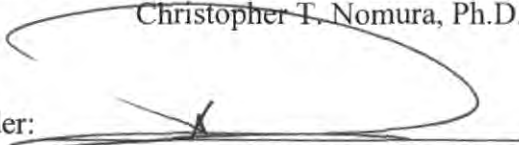
APPROVED

Thesis Project Advisor:



Christopher T. Nomura, Ph.D.

Second Reader:



Atahualpa Pinto, Ph.D.

Honors Director:



William M. Shields, Ph.D.

Date:

5/15/15

Abstract

Poly-[(*R*)-3-hydroxyalkanoates] (PHAs) are biodegradable polyesters produced by diverse microbial strains and genetically modified organisms. Increasing our understanding of different metabolic pathways within PHA-producing organisms is highly desired so as to bolster PHAs as economically competitive alternatives to petroleum-based plastics. Some pseudomonads, including *Pseudomonas putida*, *Pseudomonas aeruginosa*, and *Pseudomonas oleovorans*, commonly biosynthesize PHA polyesters composed of side chains containing between 6-14 carbons (medium chain length or MCL PHAs) derived from intracellular fatty acid feedstocks. The metabolic link between fatty acids and PHA biosynthesis is the enzyme PhaG, which was reported to exhibit 3-hydroxyacyl-ACP:CoA transferase activity. However, recent studies have suggested PhaG can alternatively function as a 3-hydroxyacyl-ACP thioesterase to produce free 3-hydroxyfatty acids which, coupled with a 3-hydroxyfatty acid:CoA ligase (AlkK), yields the CoA-activated substrates needed for polymerization by the PHA synthase, PhaC. In this study, we hypothesize that PhaG acts preferentially as a 3-hydroxyacyl-ACP thioesterase, effectively increasing the pool of free 3-hydroxyfatty acids available for their downstream CoA activation and polymerization. To test our hypothesis we cloned *phaG* (PP1408) from *P. putida* KT2440 into expression plasmids, and heterologously expressed/purified PhaG fused with either N or C terminal polyhistidine tags. To investigate the enzyme's activity *in vitro*, an *N*-acetylcysteamine (SNAC) thioester of *rac*-3-hydroxydecanoic acid was synthesized. Additionally, we are performing the enantioselective syntheses of (*R*)-3-hydroxydecanoic acid and its SNAC analog to carry out a thorough kinetic analysis of PhaG.

Table of Contents

1. Introduction	1
1.1. The Case for Biodegradable Polymers	1
1.2. Poly-[(<i>R</i>)-3-hydroxyalkanoates] (PHAs): Biodegradable Microbial Polyesters	2
2. Background	5
2.1. PhaG: The Key Link Between Fatty Acid Synthesis and PHA production.....	5
2.2. Differences in Structure and Function of Thioesterases and Acyl transferases.....	7
3. Experimental Design	9
3.1. Heterologous expression of an active PhaG-His tag fusion protein	9
3.2. Retrosynthetic Design of Enantiopure Substrates.....	10
3.3. Retrosynthetic Design of Racemic Substrate.....	11
4. Experimental Design	11
4.1. Cloning of <i>phaG</i>	11
4.2. PhaG Protein Purification	12
4.3. Synthesis	13
5. Discussion	15
6. Conclusions and Future Work	16
7. References	17
8. Supporting Information	18
General Methods and Selected NMR Spectra	18
1-Undecen-4-ol (2).....	19
Analytical Data: 1-Undecen-4-ol (2)	20
¹ H NMR: 1-Undecen-4-ol (2)	20
¹³ C NMR: 1-Undecen-4-ol (2).....	21
(4 <i>R</i>)-1-Undecen-4-ol (3)	21
Analytical Data: (4 <i>R</i>)-1-Undecen-4-ol (3).....	21
¹ H NMR: (4 <i>R</i>)-1-Undecen-4-ol (3).....	22
¹³ C NMR: (4 <i>R</i>)-1-Undecen-4-ol (3).....	23
2-(Undec-1-en-4-yloxy)tetrahydro-2 <i>H</i> -pyran (19)	23
Analytical Data: 2-(Undec-1-en-4-yloxy)-tetrahydro-2 <i>H</i> -pyran (19)	24
¹ H NMR: 2-(Undec-1-en-4-yloxy)-tetrahydro-2 <i>H</i> -pyran (19)	24
¹³ C NMR: 2-(Undec-1-en-4-yloxy)-tetrahydro-2 <i>H</i> -pyran (19)	25
3-((Tetrahydro-2 <i>H</i> -pyran-2-yl)oxy)decanal (21).....	25

Analytical Data: 3-((Tetrahydro-2 <i>H</i> -pyran-2-yl)oxy)decanal (21)	26
(<i>S</i>)-(2-Acetamidoethyl)-3-hydroxydecananethioate (17).....	26
Analytical Data: (<i>S</i>)-(2-Acetamidoethyl)-3-hydroxydecananethioate (17)	26
¹ H NMR: (<i>S</i>)-(2-Acetamidoethyl)-3-hydroxydecananethioate (17)	27
¹³ C NMR: (<i>S</i>)-(2-Acetamidoethyl)-3-hydroxydecananethioate (17).....	27

List of Figures

Figure 1. Model results showing the global distribution and density of microplastics in oceans.....	1
Figure 2. Biodegradable polyester family.....	2
Figure 3. Metabolic pathway that supply hydroxyalkanoate monomers for PHA biosynthesis.....	4
Figure 4. HPLC analysis of reaction products from enzymatic assay with PhaG.	6
Figure 5. Conversion of (<i>R</i>)-3-hydroxyacyl-ACP to (<i>R</i>)-3-hydroxyacyl-CoA.....	7
Figure 6. Serine protease mediated mechanism of a thioesterase.....	8
Figure 7. SDS-PAGE results.....	13

List of Schemes

Scheme 1. Enantiospecific retrosynthetic strategy to synthesize compounds 8 and 15	10
Scheme 2. Racemic retrosynthesis of (3)-hydroxydecanoic SNAC thioester 17	11
Scheme 3. Progress towards synthesis of enantiopure (<i>R</i>)-3-hydroxydecane SNAC thioester.....	14
Scheme 4. Model study progress to employ to enantiopure synthesis.	15
Scheme 5. Synthesis of racemic 3-hydroxydecane SNAC thioester.....	15

List of Tables

Table 1. Primers used in this study.	12
Table 2. Strains and plasmids used in this study.....	12

List of Abbreviations

3HD	3-Hydroxydecanoic acid
3HD-CoA	3-Hydroxydecanoyl CoA
ATP	Adenosine-5'-triphosphate
ACP	Acyl carrier protein
BLAST	Basic local alignment tool
BSA	Bovine serum albumin
CAL-B	Candida lipase B
CoA	Coenzyme A
DCM	Dichloromethane
DCC	<i>N,N'</i> -dicyclohexylcarbodiimide
DIPEA	Diisopropylethylamine
DMSO	Dimethylsulfoxide
DMF	Dimethylformamide
DMAP	4-Dimethylaminopyridine
DNA	Deoxyribonucleic acid
DTNB	5,5'-Dithiobis-2-nitrobenzoic acid
Et ₂ O	Diethyl ether
EtOAc	Ethyl acetate
FCC	Flash column chromatography
HPLC	High performance liquid chromatography
HSNAC	<i>N</i> -Acetylcysteamine
IPTG	Isopropyl β-D-1-thiogalactopyranoside
IPA	Isopropyl alcohol
<i>i</i> Pr ₂ O	Isopropyl ether
LB	Luria-Bertani/Lysogen broth
NAD ⁺	Nicotinamide adenine dinucleotide
NADP ⁺	Nicotinamide adenine dinucleotide phosphate
Ni-NTA	Nickel-nitriloacetic acid
NMR	Nuclear magnetic resonance
MCL	Medium chain length
OD	Optical density
PA	<i>p</i> -Anisaldehyde
PHA	Poly-[(<i>R</i>)-3-hydroxyalkanoates]
PHB	Poly-[(<i>R</i>)-3-hydroxybutyrate]
PLA	Poly-[(<i>R</i>)-3-lactic acid]
SCL	Short chain length
SDS-PAGE	Sodium dodecyl sulfate-Polyacrylamide gel electrophoresis
NAC	<i>N</i> -Acetyl cysteamine thioester
TE	Thioesterase
TEA	Triethylamine
THF	Tetrahydrofuran
THP	Tetrahydropyran
TLC	Thin layer chromatography
UV	Ultraviolet

Acknowledgements

I would like to thank the entire Nomura Research Group, especially Dr. Atahualpa Pinto for your help and support throughout this past year; Dr. Zaara Sarwar for your help with molecular techniques and protein purification; Dr. Christopher Nomura for supporting me for all four years at SUNY ESF; and Jessica Ciesla along with the rest of the lab members. I would also like to thank Dr. Bill Shields and the Honor's Program for financial support as well as the National Science Foundation (NSF CBET 126390). Lastly, I would like to thank my parents, siblings, nieces and nephews for your love and support, especially as I transition into my graduate studies.

1. Introduction

1.1. The Case for Biodegradable Polymers

Polymer degradation occurs via photochemical, mechanical and/or biological mechanisms.¹ Commonly employed petroleum-based polymers such as polyethylene, polypropylene, and polystyrene are typically degraded via photochemical and mechanical processes.² Though effective in decreasing the polymer's physical dimensions over time, these pathways do not affect its chemical character, which remains altogether intact. Nowhere is this more evident, and to a devastating degree, than in the approximately 250,000 tons of petroleum-based plastic pollution distributed across the world's ocean gyres (Fig. 1).¹ These plastic "hot-spots" have been well documented to exert deleterious effects on marine biota, from microscopic zooplankton to larger animals, resulting in ecological disturbances at different trophic levels.^{2,3}

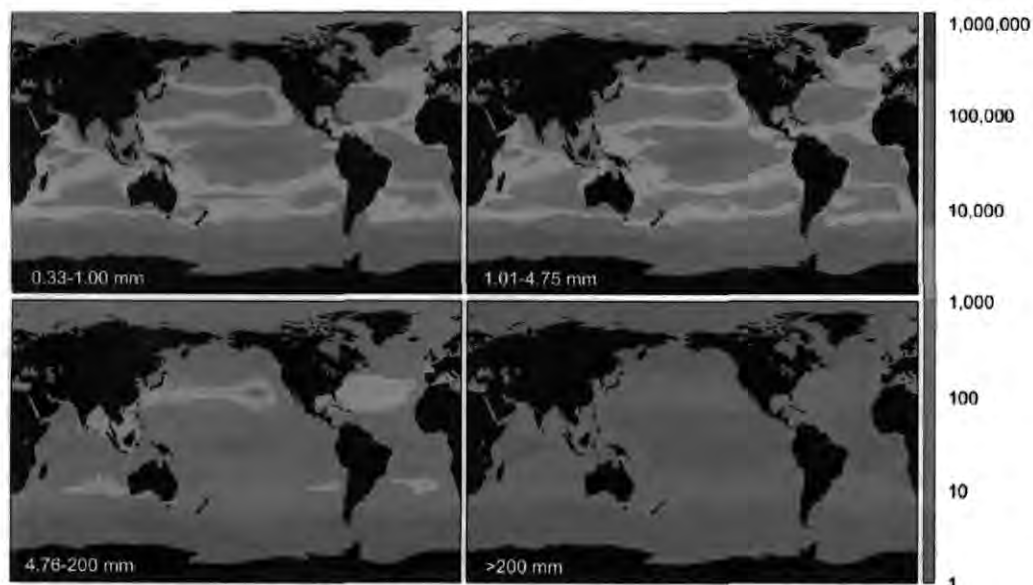


Figure 1. Model results showing the global distribution and density of microplastics in the oceans (pieces km⁻²; see colorbar), classified in four class sizes (0.33–1.00 mm, 1.01–4.75 mm, 4.76–200 mm, and >200 mm). Figure adapted from Eriksen et al., 2014³ used without permission.

Alternatively, and as opposed to non-biodegradable plastics, biodegradable polymers are fully mineralized into carbon dioxide and water through biological

mechanisms.⁴ Polymer biodegradability is dependent on the material's macromolecular structure as well as the intrinsic characteristics of the free monomers, as they must conform to the metabolic repertoire of individual organisms.¹ For example, microbes possess the appropriate enzymes (amylases) that break down starch, a natural polysaccharide, into glucose, a molecule key to their metabolic processes and survival.⁵ Other examples of polymeric materials often amenable to microbial degradation are comprised within the large family of biodegradable polyesters (**Fig. 2**), such as adipate/terephthalate, polylactic acid (PLA), and poly-[(*R*)-3-hydroxyalkanoates] (PHAs).⁵ The ester functionalities are degraded by the enzymatic action of lipases and hydrolases consequently releasing their monomeric units as organic acids, and rapidly decreasing the molecular weight and size of the polymeric particles.⁶

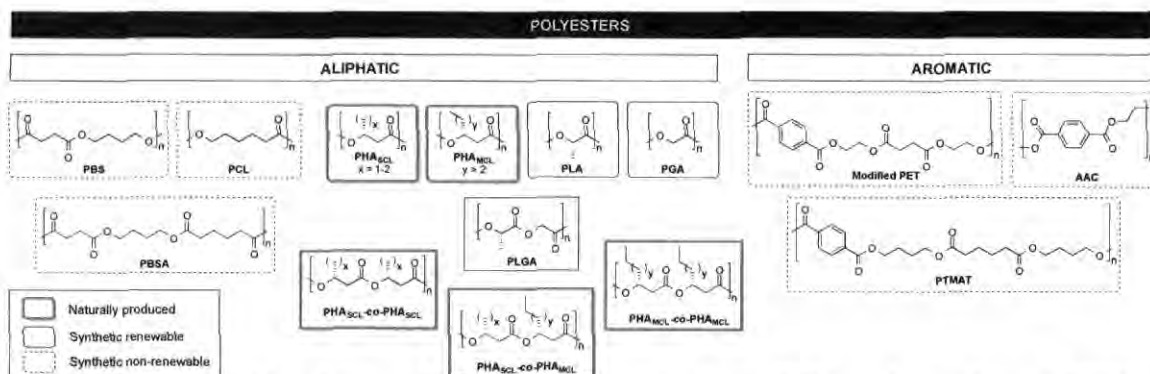


Figure 2. Biodegradable polyesters. PBS = polybutylene succinate, PCL = polycaprolactone, PBSA = polybutylene succinate adipate, PHA_{SCL} = short-chain length polyhydroxyalkanoates, PHA_{MCL} = medium-chain length polyhydroxyalkanoates, PLA = polylactic acid, PGA = polyglycolic acid, PET = polyethylene terephthalate, AAC = aliphatic–aromatic copolyesters, PTMAT = polymethylene adipate/terephthalate. Of all of the given plastics, PHAs have great potential to replace petroleum-based plastics. Figure adapted from Kasirajan and Ngouajio 2011, used without permission.⁸

1.2. Poly-[(*R*)-3-hydroxyalkanoates] (PHAs): Biodegradable Microbial Polyesters

PHAs are water insoluble inclusions within the cytoplasm of various microorganisms ranging in molecular weight from 200,000 to 3,000,000 Da.⁷ Due to the low solubility in the cytoplasm and high molecular weight, PHAs serve as carbon source

for organisms during starvation conditions.⁷ In order for PHAs to be synthesized within a bacterial cell, carbon sources (sugars/fatty acids) are enzymatically converted to (*R*)-3-hydroxyacyl-CoA intermediates, which are subsequently polymerized by a PHA synthase, or PhaC.⁷

Depending on the organism and carbon source availability, PHAs with different compositions and repeating units can be biosynthesized.⁸ For example, in *Ralstonia eutropha* the repeating units of isolated PHAs have been observed to contain 3-5 carbon atoms, consequently suggesting its cognate PhaC is specific towards short chain length (SCL) substrates.⁷ In other cases however, pseudomonads biosynthesize medium chain length (MCL) PHAs from alkanes, alkanols, or alkanates,⁹ derived from (*R*)-3-hydroxyacyl-CoA substrates ranging in size from 6 to 14 carbons in length, yielding PHAs with a wider range of structural diversity.⁷

There are three well-understood PHA biosynthetic pathways (**Fig. 3**) that take place in microorganisms.⁷ Poly-[(*R*)-3-hydroxybutyrate] (PHB) synthesis takes place by condensation of two acetyl-CoA substrates (products of glycolysis) by PhaA, a β -ketothiolase, followed by a NADPH reduction with PhaB, to produce (*R*)-3-hydroxybutyryl-CoA monomer (**Pathway I, Fig. 3**). For the production of other PHA compositions, microorganisms can alternatively increase the availability of (*R*)-3-hydroxyacyl-CoA, through the careful stereochemical tailoring of the enoyl-CoA intermediates produced during the fatty acid degradation (or β -oxidation) pathway (**Pathway II, Fig. 3**). In this pathway, CoA-activated alkyl fatty acids are oxidatively transformed to key enoyl-CoA derivatives, which function as substrates to (*S*)-specific enoyl-CoA hydratases FadB/FadJ. Likewise, PhaJ hydrates enoyl-CoA substrates but

instead it does so specifically to (*R*)-3-hydroxyacyl-CoA derivatives. These enzymes thus control the facial selectivity of water on the prochiral substrate and consequently determine their metabolic fate: either into the energy-producing transformations of the β -oxidation pathway or as substrates for PHA production (**Pathway II, Fig. 3**).⁷

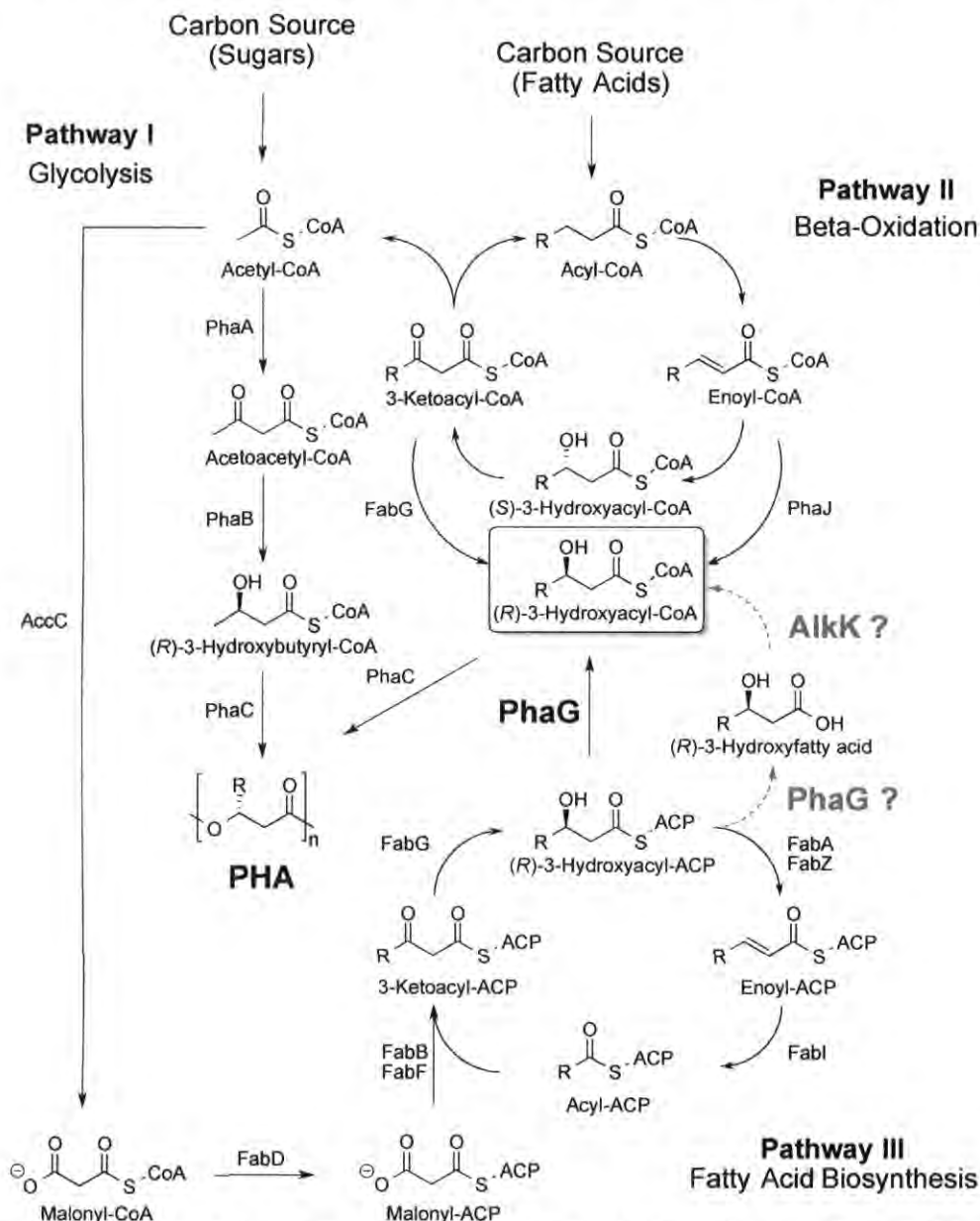


Figure 3. Metabolic pathways that supply (*R*)-3-hydroxyacyl-CoA substrates for PHA biosynthesis. Pathway I = production of PHA through acetyl-CoA from glycolysis. Pathway II = production of PHA through fatty acid breakdown via the β -oxidation pathway. Pathway III = production of PHA through fatty acid synthesis from non-fatty acid carbon sources. The latter pathway summarizes the contrasting hypotheses concerning PhaG's role in PHA production.

Lastly, PHA can also be accessed through fatty acid biosynthesis, where the enzyme PhaG plays a fundamental role.^{7,10,11} In this pathway, the fatty acyl backbone is extended by two carbons through decarboxylative condensations of malonate extender units derived from monosaccharide carbon sources. The resulting β -ketoacyl intermediates are subsequently reduced to produce fully saturated fatty acid backbones (**Pathway III, Fig. 3**).⁷ To shuttle (*R*)-3-hydroxyacyl-ACP intermediates from the fatty acid biosynthetic pathway into production of PHA, the enzyme PhaG has been identified and recognized as their fundamental link (see **Section 2.1**).⁷ The enzyme has been classified as a 3-hydroxyacyl-ACP:CoA transferase yet recent evidence has cast doubts on the validity of this classification.^{9,10} The work herein describes our rationale and approach towards describing the true role of PhaG in the biosynthesis of PHAs.

2. Background

2.1. PhaG: The Key Link Between Fatty Acid Synthesis and PHA production

To cost-effectively scaled up the fermentative production of PHAs with defined chemical compositions, the use of abundant and inexpensive feedstocks, such as sugars, is highly desirable. In 1992, Huijberts et al. showed that through *de novo* fatty acid synthesis *P. putida* KT2442 can use glucose, fructose, and glycerol to produce PHA.¹² However, the precise metabolic link driving PHA biosynthesis from sugars via fatty acid biosynthesis had remained elusive, until a study by Rehm et al. exposed the involvement of the enzyme PhaG.¹⁰ According to this study, recombinant PhaG purified from *P. oleovorans* “catalyzes the transfer of the acyl moiety from *in vitro* synthesized 3-hydroxydecanoyl-CoA to acyl carrier protein, indicating that PhaG exhibits a 3-hydroxyacyl-CoA-acyl carrier protein transferase activity.”¹⁰ Enzymatic transfer assays were completed utilizing

heterologously expressed/purified PhaG fused with an N terminal polyhistidine tag, as well as native enzyme from crude extracts, with commercially-available acyl carrier protein (ACP) and *in situ* generated *rac*-3-hydroxydecanoyl-CoA (3HD-CoA). Although assays were setup as the reverse reaction (i.e. acyltransfer from acyl-CoA to acyl-ACP), results preliminarily showed PhaG is involved (**Fig. 4**). Interestingly, controls employing saturated thioesters (octanoyl-CoA and decanoyl-CoA) showed no transfer activity, showing that PhaG is specific for 3-hydroxythioesters.¹⁰

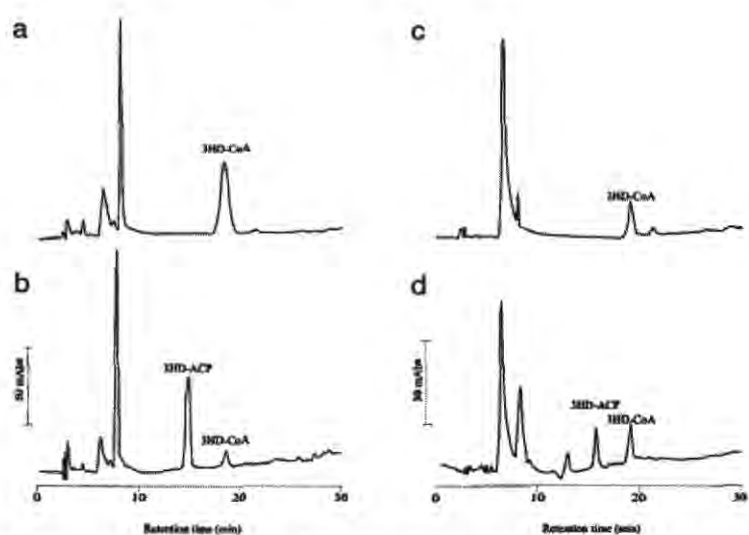


Figure 4. HPLC analysis of reaction products from enzymatic assay with PhaG. (a) Empty vector with heat inactivated PhaG (Negative control) (b) Crude PhaG extracts with 3HD-CoA (c) Heat inactivated PhaG with 3HD-CoA (negative control) (d) Purified PhaG with 3HD-CoA. Peaks were identified based on their R_f values by co-chromatography and by their spectra. Figure taken from Rehm et al. 1998 without permission.¹⁵

More recently, contradictory studies have reported the direct conversion of 3-hydroxyacyl-ACP to the corresponding 3-hydroxy fatty acids.^{10,13} Wang et al. concluded that “results suggest that PhaG functions as a 3-hydroxyacyl-ACP thioesterase to produce 3-hydroxy fatty acids.” In this study, the transcriptional levels of genes involved in fatty acid synthesis for *P. putida* KT2442 were analyzed under low/high nitrogen conditions, while grown on non-fatty acid carbon sources. This resulted in a 220-fold increase in the transcription of *phaG*, as well as 10.5-fold increase in the transcription of a putative

MCL-3-hydroxyacyl-CoA ligase (gene PP0763), suggesting that these enzymes play a key role in PHA production via *de novo* fatty acid synthesis. Wang et al. proposed that the PP0763 gene in *P. putida* encodes a putative medium-chain-fatty-acid CoA ligase similar to the AlkK enzyme from *P. oleovorans*.¹⁰ Satoh et al. described the *alkK* gene product, AlkK, as having “a relatively high specificity for medium-chain-length fatty acids.”¹⁴ PP0763 shares 36% identity and 54% similarity to AlkK from *P. oleovorans*.¹⁴ Combined, these results have elicited questions regarding the accepted mechanism in which MCL PHAs are produced from fatty acid biosynthesis by direct conversion of (*R*)-3-hydroxyacyl-ACP to (*R*)-3-hydroxyacyl-CoA. Furthermore, the results suggest that a thioesterase-mediated step is operative, and that both PhaG and AlkK cooperatively convert (*R*)-3-hydroxyacyl-ACP to (*R*)-3-hydroxyacyl-CoA, via the key (*R*)-3-hydroxyalkanoic acid intermediate (**Fig. 5**).

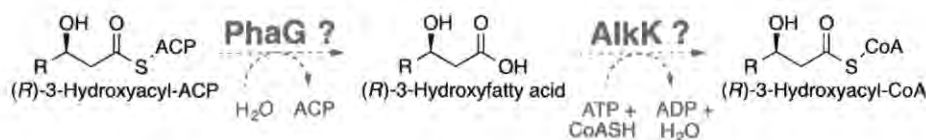


Figure 5. Proposed hypothesis of PhaG functioning as a (*R*)-3-hydroxyacyl-ACP thioesterase and AlkK functioning as a medium chain fatty acid:CoA ligase.

2.2. PhaG: A putative thioesterase involved in MCL-PHA production

Acyltransferases and thioesterases are enzyme classes belonging to the α/β hydrolase superfamily, which is characterized by a highly conserved catalytic triad consisting of Serine-Histidine-Aspartate residues (Ser-His-Asp, **Fig. 7**).¹⁵

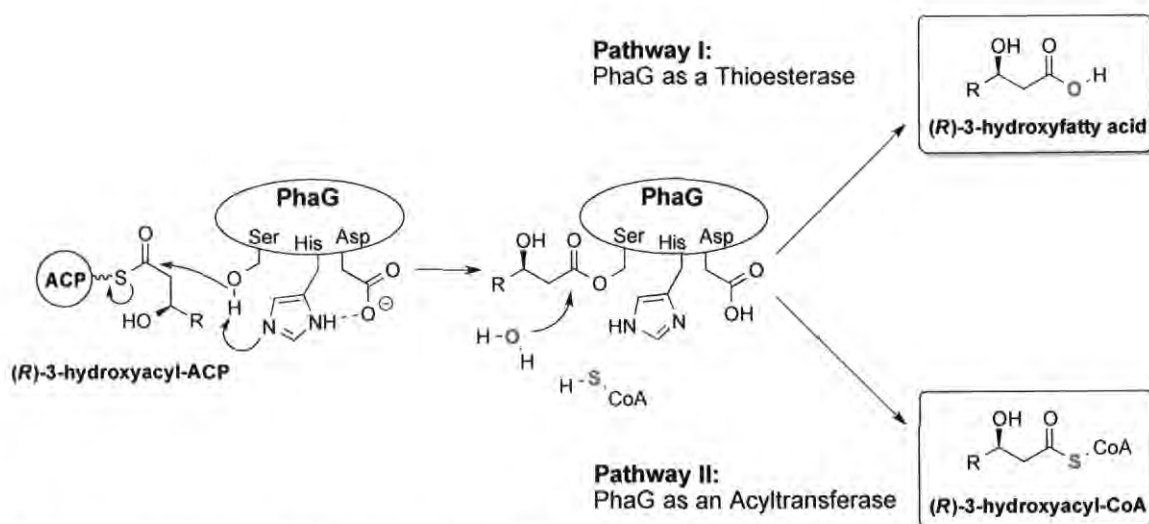


Figure 6. Mechanisms of thioesterases and acyltransferases. Characterized by a charge relay mechanism, the active site serine is first deprotonated in the loading step, and a new *O*-acyl-enzyme intermediate is formed upon its attack on an *S*-hydroxyacyl-ACP. In this charge relay mechanism, the conserved catalytic triad composed of active site Serine-Histidine-Aspartate residues attack the ACP-bound substrate yielding an enzyme-bound intermediate, which in turn is either hydrolyzed (**Pathway I**) to produce free hydroxy acid or undergoes a transthioesterification (**Pathway II**) with a CoASH substrate, affording hydroxyacyl-CoA product.

Though of a similar mechanistic paradigm, their key differentiating characteristic is acyltransferases preferentially allow attack of a nucleophile other than water (i.e. alcohols, amines, thiols) on the *O*-acyl-enzyme intermediate.¹⁶ Jiang et al. have recently studied structural differences between acyltransferases and hydrolases (thioesterases) and have identified key residues within their active sites arranged to activate their respective nucleophiles for attack. Notably, this study cautions against the use of a protein's primary sequence (via BLAST, for example) for the purpose of identifying the activity of these two enzyme classes.¹⁶ No crystal structure of PhaG has been reported/deposited in the Protein Data Bank so we have decided to take a biochemical approach to solve this problem.

The distinct structural similarities present between TEs and ATs along with the results reported by Wang et al. give reason to question whether or not PhaG has TE activity.¹¹ Furthermore, when this enzyme was first characterized (Rehm et al.), there

were no tests completed to disprove that this enzyme's TE activity.¹⁰ Additionally, Rehm et al. did not provide any mass spectrometry results from their HPLC assays nor did they provide the appropriate the co-chromatography results deciphering between apparent starting material (3HD-CoA) and product (3HD-ACP) peaks.¹⁰

Given these concerns, we hypothesize that PhaG acts preferentially as a 3-hydroxyacyl-ACP thioesterase, effectively increasing the pool of free 3-hydroxyfatty acids available for their downstream CoA activation and polymerization.

3. Experimental Design

To test our hypothesis it is necessary for PhaG to be heterologously expressed, purified and assayed for activity with an appropriate 3-hydroxyfatty acid. In this study, we describe the successful expression and purification of a C-terminal His-tagged PhaG fusion protein from recombinant *E. coli* BL21 (DE3). Additionally we demonstrate the partial synthesis of an SNAC analogue of (*R*)-3-hydroxydecanoyl-ACP, in order to carry out our enzymatic assays.

3.1. Heterologous expression of an active PhaG-His tag fusion protein

In the past, PhaG was heterologously expressed (C-terminal His-tagged) in *E. coli* JM109 and later purified by Ni-NTA chromatography.¹⁰ However, in this study, PhaG could only be isolated under denaturing conditions by and was after refolded. Additionally, PhaG was partially purified by native preparative PAGE.

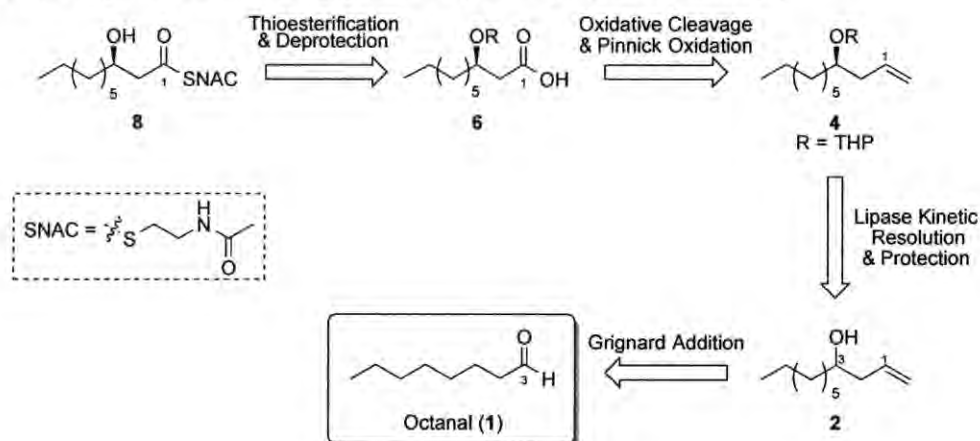
In order to test our hypothesis, we planed of expressing and purifying PhaG at a functional pH, avoiding denaturing steps. The first step for this project was to design the appropriate primers to amplify *phaG* for later expression into both C-terminal and N-terminal expression vectors. After amplification and purification, cloning of *phaG* into a

pJET cloning vector followed by cloning into the appropriate C-terminal [pET-21c(+)] and N-terminal [pET-28b(+)] expression vectors yields the appropriate plasmid constructs. Transformation into *E. coli* TOP10 and DNA purification, followed by transformation into *E. coli* BL21(DE3) yields cells that produce PhaG protein under *lac* promoter control. Large-scale growth of these cells and followed by addition of IPTG induces PhaG expression. Lysis of harvested cells by French Press, followed by addition of Ni-NTA resin to supernatants, results in the binding of His-tagged protein. Elution with imidazole EBs thereafter leads to purification of desired PhaG protein.

3.2. Retrosynthetic Design of Enantiopure Substrates

In the past, thioesters have been characterized with panels of synthetic *N*-acetylcysteamine thioesters (SNAC) to mimic the functionality of ACP thioesters.¹⁷ In order to determine the role of PhaG, a synthetic analog of (*R*)-3-hydroxyacyl-ACP will be synthesized (**8**, **Scheme 1**).

Scheme 1: Retrosynthetic analysis of (*R*)-3-hydroxydecanoyl-SNAC thioester (**8**)



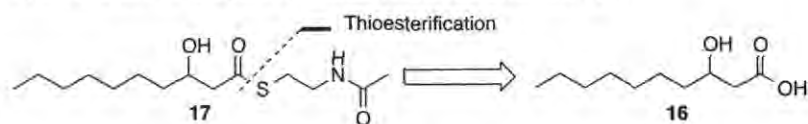
In the retrosynthetic sense, an alcohol deprotection step and hydrolytic cleavage of the chiral SNAC thioester **8** leads to protected acid **6**. Access to the latter is envisioned to arise from a key two-step sequence involving the oxidative cleavage of homoallylic

alcohol **4** followed by the adjustment of the C1 oxidation state via a Pinnick oxidation.¹⁸ Chiral protected alcohol **4** is proposed to arise from an enzymatic kinetic resolution of racemic homoallylic alcohol **2**, which will be generated by a Grignard addition to commercially available octanal (**1**).

3.3. Retrosynthetic Design of Racemic Substrate

To be able to quickly and qualitatively analyze our enzyme's activity *in vitro*, an efficient one-step synthesis was designed to access functional racemic SNAC substrate (**17**) from commercially-available *rac*-3-hydroxydecanoic acid (**16**) (Scheme 2). The route will be accomplished through a carbodiimide coupling of **16** and free HSNAC.

Scheme 2. Retrosynthesis of *rac*-3-hydroxydecanoyl-SNAC thioester (**17**)



4. Experimental Methods & Results

4.1. Cloning of *phaG*

Construction of Plasmids. The DNA region containing the putative *phaG* was amplified by PCR with the primers listed in Table 1. The gel-purified *phaG* PCR product was cloned into pJET cloning vector according to the manufacturer's instructions to yield plasmids pJGG001 and pJGG002. The *phaG* gene from pJGG001 was subcloned into the *EcoR* I/*Nde* I restriction sites of pET-21c(+) and the *phaG* gene from pJGG002 was subcloned into the *Xba* I/*EcoR* I restriction sites of pET-28b(+) to yield the respective plasmids pJGG003 and pJGG004 (Table 2). The new constructs were used to transform *E. coli* TOP10 cells. After DNA purification, sequence results verified the correct incorporation of terminal histidine tags in both cloning vectors. *E. coli* BL21 (DE3) was transformed with pJGG003 for subsequent protein expression.

Table 1. Primers used in this study

Primer	Sequence (5'-3')	Description
JG01.f	GCCAT <u>ATGAGGCCAGAAATCGCTGT</u>	Primers for <i>phaG</i> amplification with a <i>NdeI</i> site. The <i>phaG</i> sequence is underlined.
JG01.r	GCGAATTCTCAGATGGCAAATGCATGCTG	
JG02.r	GCGAATTCGCGATGGCAAATGCATGCTGCC	Primer for <i>phaG</i> amplification with an <i>EcoRI</i> site. The <i>phaG</i> sequence is underlined. JG01.f was used as the forward primer

Table 2. Strains and plasmids used in this study

Strain/Plasmid	Description	Source
<i>P. putida</i> strain KT2440	ATCC 47054	American Type Culture Collection
<i>E. coli</i> strains		
TOP10	Host for DNA cloning and manipulation	Life Technologies (Thermo Fisher Scientific)
BL21 (DE3)	Host for protein expression	New England BioLabs, Inc.
Plasmids		
pJET	A routine cloning vector for blunt end PCR products	Life Technologies (Thermo Fisher Scientific)
pET-28b(+)	A cloning vector that incorporates a N terminal polyhistidine tag	EMD Chemicals
pET-21c(+)	A cloning vector that incorporates a C terminal polyhistidine tag	EMD Chemicals
pJGG001	pJET/ <i>phaG</i> vector for subcloning into pET-21c(+)	This study
pJGG002	pJET/ <i>phaG</i> vector for subcloning into pET-28b(+)	This study
pJGG003	pET-21c(+)/ <i>phaG</i> expression vector containing a C terminal polyhistidine tag	This study
pJGG004	pET-28b(+)/ <i>phaG</i> expression vector containing a N terminal polyhistidine tag	This study

4.2. *PhaG* Protein Purification

Expression and Purification of PhaG. Expression and purification of the recombinant PhaG (C-terminal fusion protein) was performed as follows. Seed cultures were grown in LB media (supplemented with 100 µg/mL ampicillin or 100 µg/mL kanamycin) at 37°C at 200 rpm for 2 hours. These cultures were subsequently diluted 1/100 in 2x YT medium, with same concentration of appropriate antibiotics, and grown at 37°C at 200 rpm until OD₆₀₀ ~0.8 was reached. Protein expression was induced with IPTG (200 µM) followed by incubation at 16°C for 16-18 hours. Cells were harvested by

centrifugation at 3000 x g at 4°C for 30 minutes and resuspended in lysis buffer (100mM Na₃PO₄, 100 mM NaCl, pH 8.0) with lysozyme and 1 µg/mL leupeptin and pepstatin A and DNase. The suspension was lysed via French Press and after centrifugation (9000 x g at 10°C, 1 hour) and the resulting lysate was applied to a Ni-NTA resin and eluted using a gravity protein column. The elution was carried out using 20, 100 and 250 mM imidazole buffers (imidazole, 300 mM NaCl, 100 mM Tris, pH 7.5). Analysis by SDS-PAGE shows that protein at 34 kDa was eluted off in a pure fraction at 100mM imidazole (**Fig. 7**). Final protein concentration was determined by Bradford assay using a BSA calibration curve yielding 414µg/L of media.



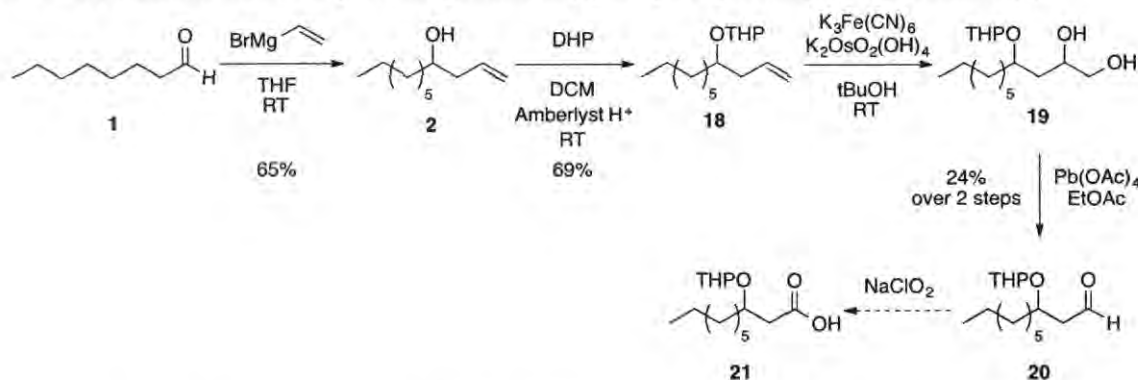
Figure 7. SDS-PAGE results. (1) SDS-Prestained Ladder. (2) Concentrated PhaG fractions. (3) 250 mM imidazole fraction. (4) 100 mM imidazole fraction #2. (5) 100 mM imidazole fraction #1. (6) 20mM imidazole fraction. (7) Original Ni-NTA column flow through. (8) Crude lysate before Ni-NTA column.

4.3. Synthesis

Route Optimization via Synthesis of Racemic Substrate Analogs. To optimize the chemistry involved in the synthesis of enantiopure substrate **8**, a model racemic synthesis was concomitantly explored and partially completed (**Scheme 3**). Three specific and key transformations in our proposed route are of concern and in need of

optimization: the kinetic resolution of **2** (for details, see **Scheme 4**), the oxidative cleavage of alkene **18**, and its oxidation to carboxylic acid **21** via a Pinnick oxidation.¹⁸ Intermediate **2** was subsequently protected with 3,4-dihydro-2*H*-pyran (DHP) in the presence of Amberlyst® 15 cationic resin in DCM at room temperature to generate tetrahydropyranyl ether (THP) **18** at 69% yield. The protected alcohol was dihydroxylated employing Sharpless conditions [$K_3Fe(CN)_6$, $K_2OsO_2(OH)_4$] to afford vicinal diol **19** which was treated with $Pb(OAc)_4$ in EtOAc at room temperature for 10 minutes to furnish aldehyde **20** (24% yield over two steps).¹⁹ Due to the low yielding steps from alkene **18** to aldehyde **20**, we have begun exploring, with great success, the ozonolysis of racemate **18** (not shown). With aldehyde **20** in hand, an often-predictable Pinnick oxidation should lead to acid **21**, a stable intermediate in the synthesis of our desired SNAC thioester analog. By exploring key reactions through the use of racemic intermediates, we have thus gained confidence in their applicability to the synthesis of enantioenriched substrates.

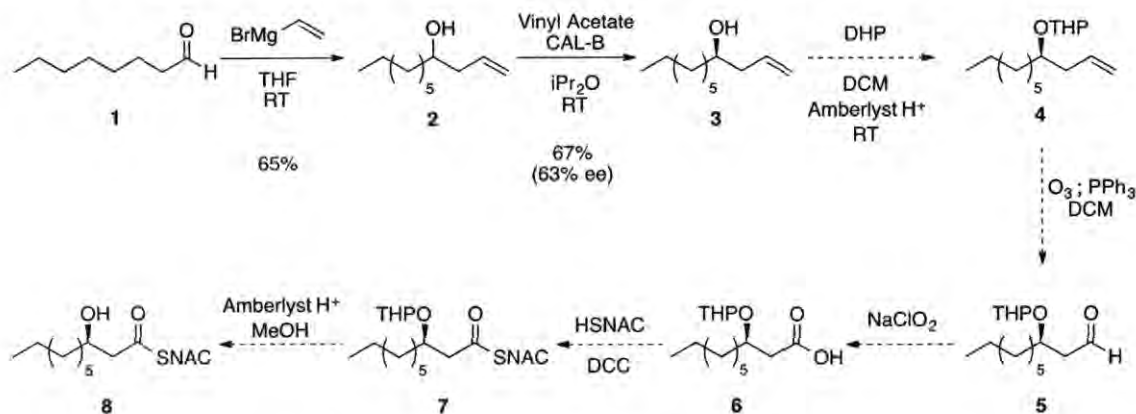
Scheme 3. Racemic model study for the synthesis of (*R*)-3-hydroxydecanoyl-SNAC thioester (**8**)



Synthesis of (*R*)-3-hydroxydecanoyl-SNAC Thioester (8**).** Synthesis of enantiopure (*R*)-3-hydroxy SNAC thioester **8** has been partially completed. Racemic 1-undecen-4-ol (**2**), was obtained by reaction of commercially available octanal (**1**) with

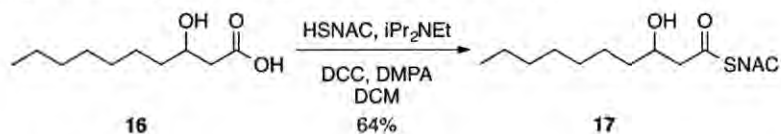
vinyl magnesium bromide in Et₂O at 0°C in 65% yield.¹⁹ Access to (4*R*)-1-undecen-4-ol (3), was attempted by performing an enzymatic kinetic resolution of 1-undecen-4-ol (2) with lipase B from *Candida antarctica* (CAL-B).²⁰ Treatment of homoallylic alcohol 2 with vinyl acetate in *i*Pr₂O, at room temperature, provided 3 in 65% yield and 63% *ee* (Scheme 4).²⁰

Scheme 4. Progress towards the synthesis of (*R*)-3-hydroxydecanoyl-SNAC thioester (8).



Synthesis of *rac*-3-hydroxydecanoyl-SNAC Thioester (17). Synthesis of the racemic 3-hydroxydecanoyl-SNAC thioester 17 has been completed. *Rac*-3-hydroxydecanoic acid 16 was dissolved in anhydrous DCM at room temperature and DCC, DIPEA, and DMAP coupling reagents were added, following addition of HSNAC. After purification this reaction resulted in a 64% yield (Scheme 5).¹⁸

Scheme 5. Synthesis of *rac*-3-hydroxydecanoyl-SNAC thioester (17).



5. Discussion & Conclusions

Based on transcription levels of *phaG* and gene PP0763 during PHA production in *P. putida* KT2442, as well the accumulation of 3HD in recombinant *E. coli* with over expressed *phaG*, we believe that PhaG preferentially acts as a thioesterase rather than an

ACP:CoA acyl transferase.¹⁶ Due to the lack of concrete evidence in support of the AT activity of PhaG, we believe that it is necessary to further probe the activity of this enzyme.¹⁵ Design of primers JG01.f, JG01.r and JG02.r led to the successful amplification of *phaG* and correct incorporation into expression vectors yielding pJGG003 and pJGG004. The constructed expression vector, pJGG003 led to expression of PhaG, which was then successfully purified through Ni-NTA chromatography, giving the first procedure to purify active PhaG at a functional pH. Synthesis of *rac*-3-hydroxydecanoyl SNAC thioester afforded the correct substrate to carry out biochemical and kinetic assays. Preliminary results using DTNB as a colorimetric agent, detecting release of free thiol, appear to support our hypothesis (not reported). Upon optimization of biochemical and kinetic assays, an accurate and precise profile of PhaG will be developed to once and for all settle the controversy surrounding this imperative enzyme.

6. Future Work

To complete this study there are a few experiments that need to be carried out to definitively define PhaG. Most importantly, this includes completion of the biochemical and kinetic assays. Currently, efforts are being made to optimize the biochemical reaction conditions, as well as a spectroscopic procedure to detect starting material and product. Ideally, we will be able to obtain mass spectrometry results from these assays to undisputedly determine the enzyme products. Once this is established a kinetic profile utilizing the Michaelis-Menten kinetic model will be generated. Additionally, we would like to express purify halo-ACP to test if PhaG also conducts transferase activity. If this were the case, we would employ both the SNAC substrate along with halo-ACP to test if there is a preferential reaction for PhaG with both substrates available. Lastly, much work

needs to be completed to finish the synthesis of enantiopure SNAC substrates. In order for this to be an obtainable goal, it is crucial to optimize the lipase resolution step, ideally giving an *ee* of 90% or higher.

7. References

- (1) Eriksen, M.; Lebreton, L. C. M.; Carson, H. S.; Thiel, M.; Moore, C. J.; Borerro, J. C.; Galgani, F.; Ryan, P. G.; Reisser, J. *PLoS ONE* **2014**, *9* (12)
- (2) Andrady, A. L. *Mar. Pollut. Bull.* **2011**, *62*, 1596–1605.
- (3) Rios, L. M.; Moore, C.; Jones, P. R. *Mar. Pollut. Bull.* **2007**, *54*, 1230–1237.
- (4) Andrady, A. L. *J. Macromol. Sci.* **1994**, *34* (1), 25–75.
- (5) Hanes, C. S. *Proc. R. Soc. Lond. [Biol.]* **1940**, *128* (853), 421–450.
- (6) Bachmann, B. M.; Seebach, D. *Macromolecules* **1999**, *32* (6), 1777–1784.
- (7) Sudesh, K.; Abe, H.; Doi, Y. *Prog. Polym. Sci.* **2000**, *25*, 1503–1555.
- (8) Tappel, R. C.; Kucharski, J. M.; Mastroianni, J. M.; Stipanovic, A. J.; Nomura, C. T. *Biomacromolecules* **2012**, *13* (9), 2964–2972.
- (9) Lageveen, R. G.; Huisman, G. W.; Preusting, H.; Ketelaar, P.; Eggink, G.; Witholt, B. *Appl. Environ. Microbiol.* **1988**, *54*, 2924–2932.
- (10) Rehm, B. H. A.; Krüger, N.; Steinbüchel, A. *J. Biol. Chem.* **1998**, *273*, 24044–24051.
- (11) Wang, Q.; Tappel, R. C.; Zhu, C.; Nomura, C. T. *Appl Environ Microbiol* **2012**, *78*, 519–527.
- (12) Huijberts, G. N.; Eggink, G.; Waard, P. de; Huisman, G. W.; Witholt, B. *Appl. Environ. Microbiol.* **1992**, *58* (2), 536–544.
- (13) Zheng, Z.; Zhang, M.-J.; Zhang, G.; Chen, G.-Q. *Antonie Van Leeuwenhoek* **2004**, *85* (2), 93–101.
- (14) Satoh, Y.; Murakami, F.; Tajima, K.; Munekata, M. *J. Biosci Bioeng.* **2005**, *99*, 508–511.
- (15) Schreck, S. D.; Grunden, A. M. *Appl. Microbiol. Biotechnol.* **2014**, *98* (3), 1011–1021.
- (16) Jiang, Y.; Morley, K. L.; Schrag, J. D.; Kazlauskas, R. J. *ChemBioChem* **2011**, *12*, 768–776.
- (17) Pinto, A.; Wang, M.; Horsman, M.; Boddy, C. N. *Org. Lett.* **2012**, *14* (9), 2278–2281.
- (18) Bal, B. S.; Childers Jr., W. E.; Pinnick, H. W. *Tetrahedron* **1981**, *37* (11), 2091–2096.
- (19) Donohoe, T. J.; Sintim, H. O. *Org. Lett.* **2004**, *6* (12), 2003–2006.
- (20) Das, T.; Bhuniya, R.; Nanda, S. *Tetrahedron: Asymmetry* **2010**, *21* (18), 2206–2211.

8. Supporting Information

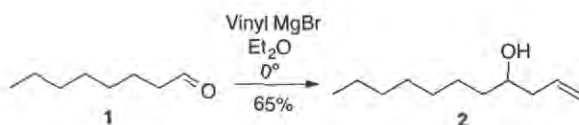
General Molecular Biology Methods. DNA was purified using Promega (Madison, WI) nucleic acid purification kits. Restriction enzymes and ligases were products of New England BioLabs (Ipswich, MA). PrimeStar polymerase (TaKaRa Biosciences, Japan) was used for all PCR reactions. PCR amplifications were done, following the recommended protocols for the Prime-Star polymerase protocol. All ligation processes were completed with T4 DNA ligase (NEB) and essential sequences verified by GENEWIZ Inc.

General Synthetic Methods. Reactions were carried out under an argon atmosphere with dry solvents and oven-dried glassware under anhydrous conditions unless specified otherwise. Tetrahydrofuran (THF), dichloromethane (DCM), dimethylsulfoxide (DMSO) and dimethylformamide (DMF) were purchased and employed without further purification. Solvents such as ethyl acetate (EtOAc) and hexanes, employed in workup and chromatographic separations, were used without further purification, unless otherwise stated. Brine refers to a saturated aqueous solution of sodium chloride (NaCl). Reagents were purchased at the highest commercial quality and used without further purification, unless otherwise stated. Yields refer to chromatographically and spectroscopically (^1H and ^{13}C NMR) homogeneous materials, unless otherwise stated. Reactions were monitored by analytical thin-layer chromatography (TLC) and carried out on 250 μm E. Merck silica gel plates (60F-254) using UV light as the visualizing agent and an acidic solution of *p*-anisaldehyde (PA) and heat, or ninhydrin and heat as developing agents. Flash column chromatography was performed with SiliCycle SiliaFlash F60 silica gel (pore size 60 Å, particle size 40-63

μm). NMR spectra were recorded on Bruker AVANCE III HD 800 MHz and Bruker AVANCE III 600 MHz instruments, and were calibrated using residual undeuterated solvents as internal reference (chloroform, $\delta = 7.26$ ppm, ^1H NMR; 77.0 ppm, ^{13}C NMR; dimethylsulfoxide, $\delta = 2.50$ ppm, ^1H NMR; 39.52 ppm, ^{13}C NMR). Chemical shifts (δ) are reported in parts per million (ppm); NMR peak multiplicities are denoted by the following abbreviations: s = singlet, d = doublet, t = triplet, q = quartet, p = pentet, dd = doublet of doublets, dt = doublet of triplets, m = multiplet, br = broad; coupling constants (J) are reported in Hertz (Hz).

Experimental Procedures and Selected NMR Spectra

1-Undecen-4-ol (2)



To a 250 mL round-bottom flask, 4.11 g (32.1 mmol) of octanal (1) was dissolved in Et_2O (62 mL) and was cooled to 0 °C while under an argon atmosphere. To this, vinyl magnesium bromide solution (34 mL, 1.0 M in Et_2O) was added slowly while monitoring the exotherm. The reaction was allowed to warm to room temperature overnight and was then deemed complete via TLC. The reaction was cooled back down to 0°C and quenched with an aqueous saturated solution of ammonium chloride (NH_4Cl , 20 mL) and water (20 mL). The layers were separated and the aqueous was extracted with EtOAc (3 x 100 mL). The combined EtOAc extractions were washed with brine (3 x 100 mL) and subsequently dried over anhydrous MgSO_4 . The mixture was filtered through a 100 mL fritted glass funnel and the filter cake was washed with 50 mL of EtOAc . The filtrate was concentrated in vacuo to afford a crude yellow oil (5.01 g, 29.4 mmol, 92%). The oil was

purified by silica column chromatography (6% EtOAc/hexanes) to yield a clear pure oil (3.55 g, 20.9 mmol, 65%).

Analytical data for 2^a

M.W.: 170.29 g/mol

TLC (R_f): 0.575 (10% EtOAc/hexanes): PAA Stain

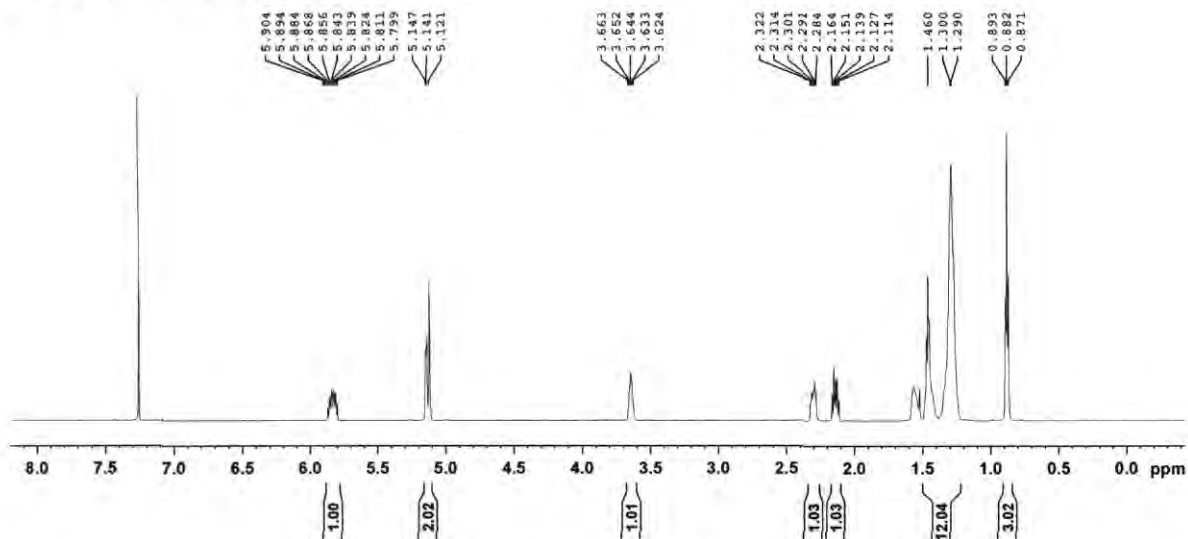
¹H NMR: (600 MHz, CDCl₃)
δ 5.90-5.80 (m, 1 H), 5.15-5.12 (m, 2 H), 3.66-3.62 (m, 1H), 2.32-2.28 (m, 1 H), 2.16-2.11(m, 1 H) 1.50-1.44 (m, 12 H), 0.87-0.89 ppm (t, 1 H, J= 6.6Hz).

¹³C NMR: (150 MHz, CDCl₃)
δ 134.95, 118.01, 70.73, 41.99, 36.86, 31.84, 29.61, 29.27, 25.67, 22.65, 14.08 ppm

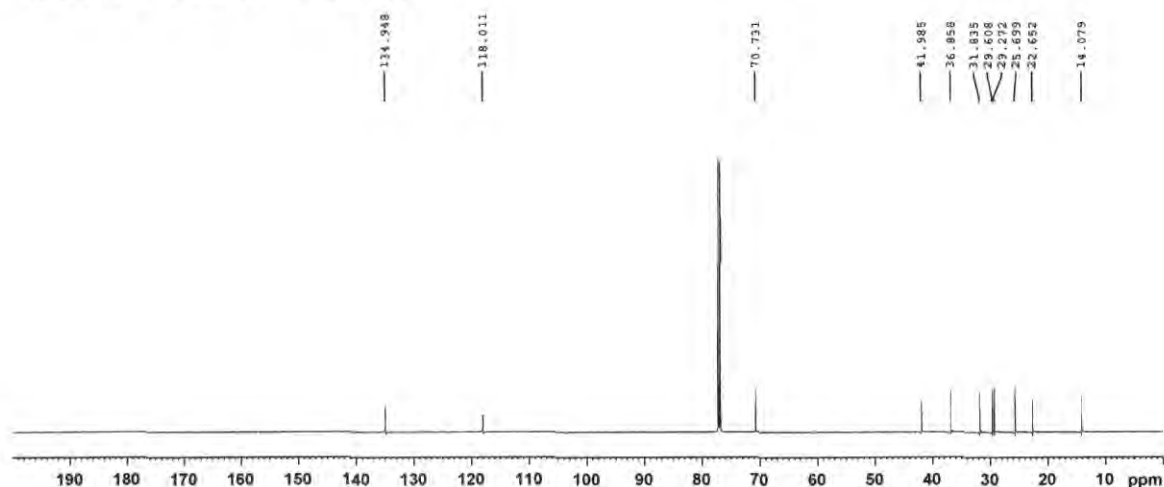
Reference: Donohoe, T. J.; Sintim, H. O. *Org. Lett.* **2004**, 6 (12), 2003–2006.

^a Alcohol **2** was identical to its previously reported spectroscopic values

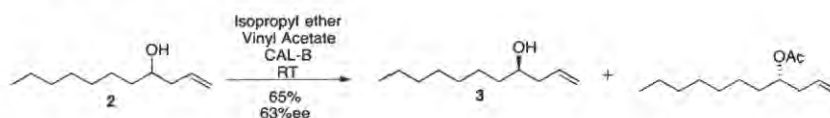
¹H NMR: 1-Undecen-4-ol (**2**)



¹³C NMR: 1-Undecen-4-ol (2)



(4*R*)-1-Undecen-4-ol (3)



To a 25 mL round-bottom flask, 204 mg (1.2 mmol) of 1-Undecen-4-ol (2), 103 mg (1.2 mmol) of vinyl acetate and 48 mg of CAL-B were dissolved in *i*Pr₂O (3.6 mL). This was allowed to shake at room temperature on Recipro-Shaker at 154 min⁻¹. The reaction was monitored by GC and deemed complete after 21 hours (1:1 ratio of products), filtered and concentrated in vacuo to give a crude oil. The oil was purified by silica column chromatography at 20% EtOAc/hexanes to give 66 mg (3.88 mmol, 65%) of pure alcohol. Optical rotation gave a value of +0.220° (4.4 g/100mL) giving an *ee* of 63%.

Analytical data for 3^a

M.W.: 170.29 g/mol

TLC (*R_f*): 0.575 (10% EtOAc/hexanes): PAA Stain

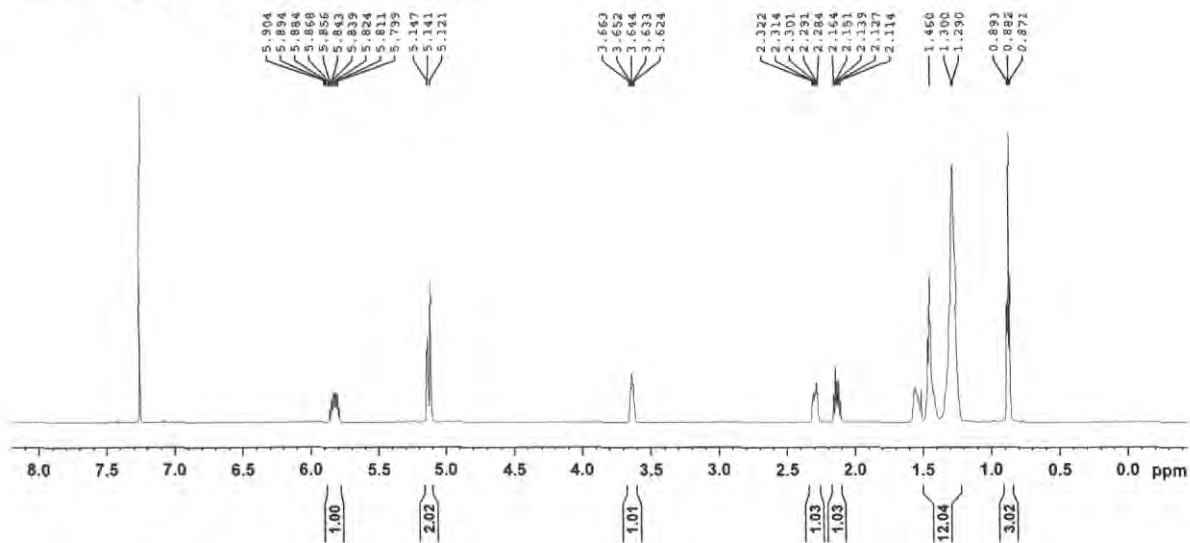
¹H NMR: (600 MHz, CDCl₃)
δ 5.90-5.80 (m, 1 H), 5.15-5.12 (m, 2 H), 3.66-3.62 (m, 1H),
2.32-2.28 (m, 1 H), 2.16-2.11(m, 1 H) 1.50-1.44 (m, 12 H), 0.87-
0.89 (t, 1 H, *J* = 6.6Hz) ppm.

¹³C NMR: (150 MHz, CDCl₃)
δ 134.95, 118.01, 70.73, 41.99, 36.86, 31.84, 29.61, 29.27,
25.67, 22.65, 14.08 ppm.

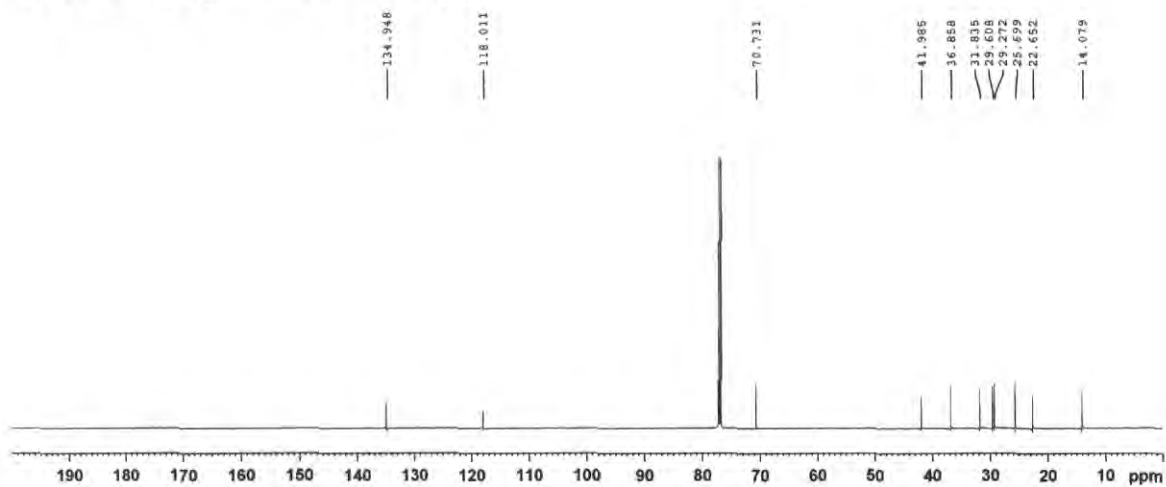
Reference: Feng, J.-P.; Shi, Z.-F.; Li, Y.; Zhang, J.-T.; Qi, X.-L.; Chen, J.;
Cao, X.-P. *J. Org. Chem.* **2008**, *73* (17), 6873–6876

^a Alcohol **3** was identical to its previously reported spectroscopic values

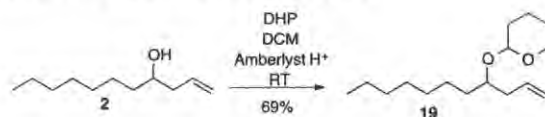
¹H NMR: (4*R*)-1-Undecen-4-ol (**3**)



¹³C NMR: (4*R*)-1-Undecen-4-ol (**3**)



2-(Undec-1-en-4-yloxy)tetrahydro-2H-pyran (**19**)



To a 25 mL round-bottom flask, 50 mg (0.29 mmol) of 1-Undecen-4-ol (**2**) was dissolved in DCM (0.5 mL) and was stirred at room temperature while under an argon atmosphere. To this, 10 mg of Amberlyst®15 cation exchange resin was added followed by 29 mg of 3,4-dihydropyran (0.35 mmol, DHP). The reaction was allowed stir at room temperature overnight and was then deemed complete via TLC. The reaction was filtered and the filtrate was concentrated in vacuo to afford a crude yellow oil. The oil was purified by silica column chromatography (3% EtOAc/hexanes) to yield a mixture of diastereomers as a yellow oil (51.2 mg, 0.201 mmol, 69%). It is important to note that there are unknown few peaks in both the ^1H NMR and ^{13}C NMR that do not correspond to **19**. Additionally, there are no spectral references of **19** to compare.

Analytical data for **19**

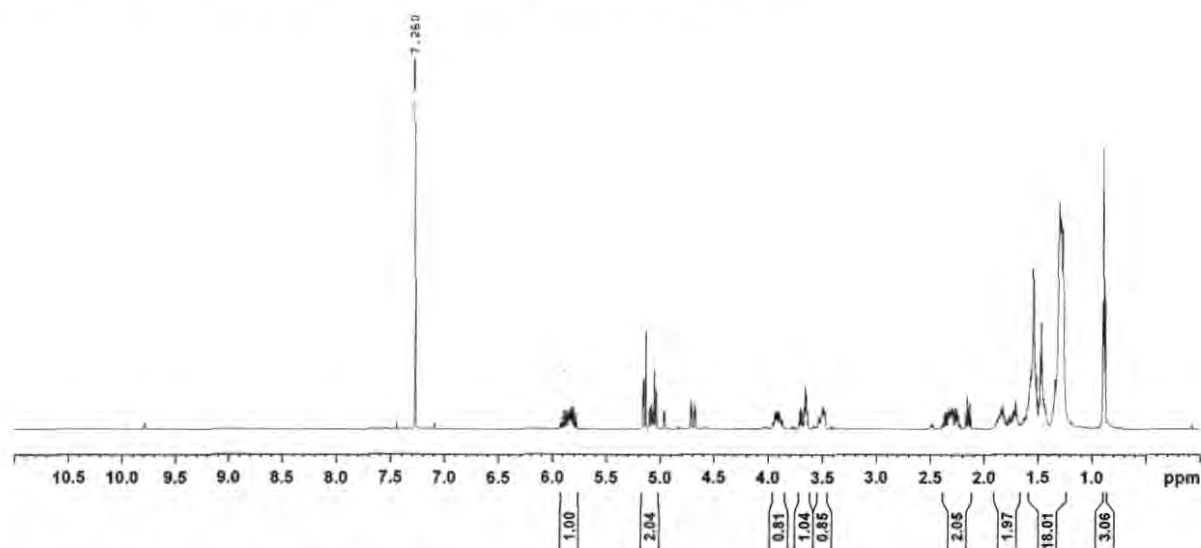
M.W.: 254.41 g/mol

TLC (*R_f*): 0.29 & 0.27 (5% EtOAc/hexanes): PAA Stain

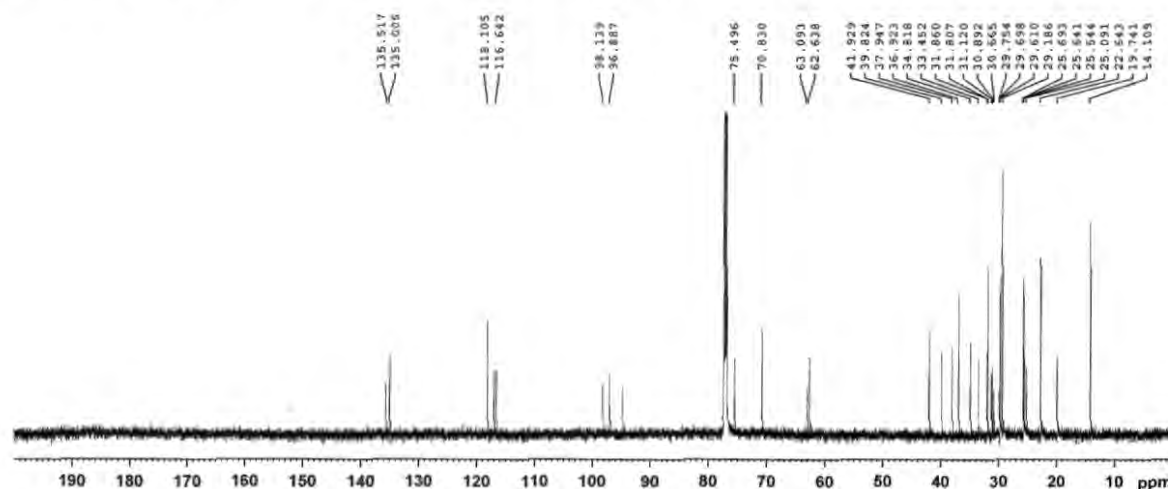
^1H NMR: (600 MHz, CDCl_3)
 δ 5.92-5.75 (m, 1 H), 5.15-5.04 (m, 2 H), 3.95-3.83 (m, 1H), 3.71-3.61 (m, 1 H), 3.55-3.45 (m, 1 H), 2.40-2.11 (m, 2 H) 1.91-1.57 (m, 2 H), 1.50-1.19 (m, 18 H), 0.87-0.89 ppm (m, 3 H).

^{13}C NMR: (150 MHz, CDCl_3)
 δ 135.52, 135.01, 118.11, 116.64, 98.14, 96.89, 75.50, 70.83, 63.09, 62.64, 41.93, 39.82, 37.95, 36.92, 34.82, 33.45, 31.86, 31.80, 31.12, 30.89, 30.67, 29.75, 29.70, 29.61, 29.19, 25.69, 25.64, 25.54, 25.09, 22.64, 19.74, 14.11ppm

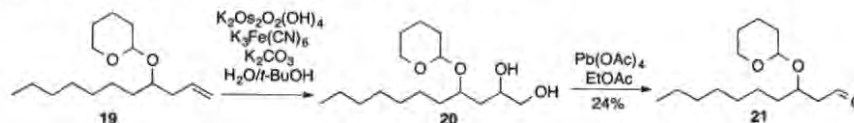
¹H NMR: 2-(undec-1-en-4-yloxy)tetrahydro-2H-pyran (**19**)



¹³C NMR: 2-(undec-1-en-4-yloxy)tetrahydro-2H-pyran (**19**)



3-((Tetrahydro-2H-pyran-2-yl)oxy)decanal (**21**)



A solution of **19** (25 mg, 0.098 mmol) in 0.25 mL of H_2O and 0.25 mL of $t-BuOH$ was treated with potassium ferricyanide ($K_3Fe(CN)_6$, 96.8 mg, 0.294 mmol), potassium carbonate (K_2CO_3 , 40.6 mg, 0.294 mmol) and $K_2Os_2O_2(OH)_4$ (1 mg, 2.5 mol %). The resulting solution was stirred at room temperature for 18 hours before being deemed

complete by TLC. To the reaction, 2 mL of both H₂O and EtOAc were added and the layers were subsequently separated. The aqueous was extracted 3 x 15 mL of EtOAc and pooled. The organics were washed 2 x 50 mL of brine and dried over Mg₂SO₄, filtered and concentrated to give the diol as a brown oil. The oil was run through a small plug of silica and eluted with 60 % EtOAc/hexanes to give a clear oil (**20**).

The diol was dissolved in 3 mL of EtOAc and treated with 51.65 mg (0.1164 mmol) of Pb(OAc)₄ and stirred at room temperature under argon for ten minutes. The reaction was deemed complete by TLC and was filtered through 30 mL of silica using 100 mL of 50% EtOAc/hexanes. The filtrate was washed 1 x 50 mL of satd NaHCO₃, 1 x 50 mL of brine, dried over Mg₂SO₄, filtered and concentrated to give 10 mg of a yellow oil. The aldehyde was purified by silica column chromatography (10% EtOAc/hexanes) to yield 6 mg (0.23 mmol, 24 %) of a clear oil.

Analytical data for **21**

M.W.: 256.39g/mol

TLC (R_f): 0.58 (20% EtOAc/hexanes): PA Stain

(S)-(2-Acetamidoethyl)-3-hydroxydecanethioate (17)



In a 5 mL vial, 10 mg (0.05 mmol) of racemic 3-hydroxydecanoic acid (**16**) was dissolved in 2.0 mL of DCM and treated with 1 mg (0.005 mmol) of DMAP, 17 mg (0.08 mmol) of DCC, 8 mg (0.06 mmol) of DIPEA, and 7 mg (0.06 mmol) of HSNAC at room temperature for 18 hours. Reaction was deemed complete by TLC and was evaporated to

dryness. Thioester product (**17**) was purified by silica column chromatography (3% MeOH/DCM) to afford 9.6 mg of a clear oil (0.032 mmol, 64 %).

Analytical data for **17**^a

M.W.: 289.43 g/mol

TLC (*R_f*): 0.24 (10% MeOH/DCM: PAA Stain)

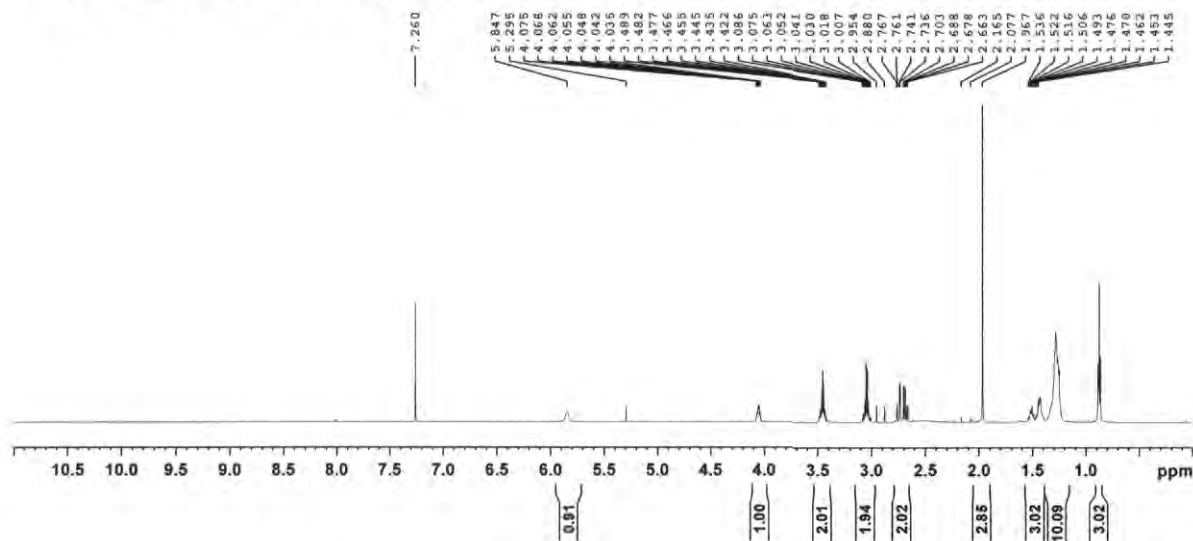
¹H NMR: (600 MHz, CDCl₃)
δ 5.85 (bs, 1H), 4.08-4.04 (m, 1H), 3.49-3.42 (m, 2H), 3.09-3.01 (m, 2H), 2.77-2.66 (m, 2H), 1.96 (s, 3H), 1.52-1.37 (m, 3H), 1.38-1.21 (m, 10H), 0.88 (t, 3H, *J* = 6.6 Hz) ppm.

¹³C NMR: (150 MHz, CDCl₃)
δ 199.59, 170.48, 69.03, 51.01, 39.32, 36.74, 31.84, 29.45, 29.19, 28.80, 25.48, 23.17, 22.60, 14.05 ppm

Reference: Schwab, J. M.; Habib, A.; Klassen, J. B. *J. Am. Chem. Soc.* **1986**, *108* (17), 5304–5308

^a **17** was identical to its previously reported spectroscopic values

¹H NMR: *S*-(2-acetamidoethyl)-3-hydroxydecanethioate (**17**)



¹³C NMR: *S*-(2-acetamidoethyl)-3-hydroxydecanethioate (17)

